Temporal-autoencoding neural network revealed the underlying functional dynamics of fMRI data: Evaluation using the Human Connectome Project data

Jong-Hwan Lee[1,2], Eric C. Wong[3], and Peter Bandettini[2]

[1]Department of Brain and Cognitive Engineering, Korea University, Seoul, Korea, Republic of, [2]Section on Functional Imaging Methods, Laboratory of Brain and Cognition, National Institute of Mental Health, National Institutes of Health, Bethesda, MD, United States, [3]Department of Radiology, University of California, San Diego, La Jolla, CA, United States

Synopsis

We proposed a novel approach based on a temporal autoencoding neural network (TANN) model to predict the fMRI volume in the next time point or repetition time (TR) based on the fMRI volume in the present TR. Using motor task data from the Human Connectome Project, our TANN model revealed the human motor cortex dynamics. The highly task-specific foot, hand, and tongue networks within the motor-related areas were clearly identified from the TANN weight features and the task-associated networks across the frontal, parietal, temporal, and visual areas were also clearly parcellated without any task information.

Introduction

Interpretation of functional neuroimaging data of the human brain is important to understand the underlying cognitive processes. For example, the dynamic functional connectivity (FC) analysis using a sliding window has been shown the temporal evolution of the neuronal connectivity patterns [1], however, the underlying relationship between consecutive whole-brain fMRI volumes has not been explicitly explored. Here, we proposed a novel approach based on a temporal autoencoding neural network (TANN) model to predict the fMRI volume in the next time point or repetition time (TR) by using the fMRI volume in the present TR.

Materials and Methods

Figure 1 shows the (a) proposed TANN architecture and (b) training algorithm. The motor task fMRI runs of the Human Connectome Project (HCP) [2] were used to evaluate the TANN. All the input samples were repeatedly used 300 times (i.e. epochs) with a momentum strength of 0.5 [3]. The weights were updated in every 200 input samples using Eq. (3) of Fig. 1b. The η in Eq. (3) was initially 0.005 and gradually reduced to 0.00066 at 300 epochs; α in Eq. (2) was adaptively changed between 0 and 0.01 [4,5]; β in Eq. (2) was fixed to 10^{-5}. The MATLAB codes implementing an autoencoding network (http://bspl.korea.ac.kr) were modified and multiple Linux machines (Intel i7; > 3GHz CPU; > 64GB RAM) were used to train the TANN model for each of two levels of the weight sparsity (i.e. Hoyer's sparseness [6] of 0.5 and 0.7) and using smoothed or unsmoothed HCP fMRI volumes.

Once the TANN training was finished, the sign of the paired encoding/decoding features $W^e_{(i)}$ and $W^d_{(i)}$ associated with the ith hidden node was changed, so that the skewness of $W^d_{(i)}$ becomes positive [7]. The highly task-specific $W^d_{(i)}$ were visualized using the "wb_view" tool and the time-series of the ith hidden node output corresponding to the input fMRI volume series were analyzed.

Results

Fig. 2 shows the learning curves of the TANN training (took approximately 7 hours using the Linux computer: Intel i7-6700 3.4GHz CPU, 64GB RAM, and Ubuntu-16). The encoding/decoding weights from 82 hidden nodes out of 100 are localized within the brain area. The encoding/decoding features from the 18 remaining hidden nodes showed pseudo-randomly distributed spatial patterns which might be learnt to estimate thermal noises of the input fMRI volumes. Figs. 3 and 4 show the five most task-specific $W^d_{(i)}$ and the time-series of the corresponding i^{th} hidden node output, respectively.

Fig. 5 shows the pairs of $W^d_{(i)}$, in which the output time-series of the corresponding hidden nodes are highly correlated. These pairs of hidden nodes are co-active along the task fMRI run and thus may reveal the functional dynamics associated with the task across the whole brain. For example, in (a), the foot-areas related hidden nodes showed the slightly greater ipsilateral activations from the left-toe than right-toe clenching task periods (i.e. at approximately 50 and 170 TRs). In (b), the visuo-motor (3) and parieto-motor (4) related hidden nodes were substantially active during the motor task periods, whereas these hidden nodes were quiet during the fixation/rest periods (i.e. 10, 140, 220, and 275 TRs). Interestingly, the hidden node (5) that represents the left superior-parietal/supramarginal, inferior temporal, inferior precentral, middle frontal areas are substantially co-active with multiple nodes that represent the bilateral precuneus (6 in c), left insula and its proximity (16 in d), and superior frontal and dorsal anterior cingulate (14 in f). In (g), the medial (12) and lateral (13) parts of the secondary visual cortices were separated into two hidden nodes and these networks are tightly co-active whenever visual cues were presented across the 13 blocks (i.e. the 10 motor and 3 fixation blocks).

Discussion

Our proposed computational neural network model revealed the human motor cortex dynamics in the HCP data. The highly task-specific foot, hand, and tongue networks were clearly identified from the decoding weights and the task-associated networks across the frontal, parietal, temporal, and visual areas were also clearly separated. The validity of these networks was supported by the temporal evolution of the associated hidden nodes. These functionally-parcellated networks from our TANN model and the associated time-series are currently examined such as comparing the results from alternative data-driven methods including ICA that would not reveal multiple components with highly correlated time-courses in the medial/lateral visual cortices (Fig. 5g).

Conclusion

The proposed computational model appears to extract the underlying functional dynamics of each individual fMRI run without any task information. It is thus straightforward to apply this model to other sensory/motor/cognitive tasks and resting-state fMRI data.

Acknowledgements

References

1. Hutchison RM, Womelsdorf T, Allen EA, et al. Dynamic functional connectivity: promise, issues, and interpretations. NeuroImage. 2013;80:360-378.

2. Glasser M, Coalson T, Robinson E, et al. A Multi-modal parcellation of human cerebral cortex. Nature. 2015.

3. LeCun YA, Bottou L, Orr GB, Müller K-R. Efficient backprop. Neural networks: Tricks of the trade: Springer; 2012:9-48.

4. Kim J, Calhoun VD, Shim E, Lee J-H. Deep neural network with weight sparsity control and pre-training extracts hierarchical features and enhances classification performance: Evidence from whole-brain resting-state functional connectivity patterns of schizophrenia. NeuroImage. 2016;124:127-146.

5. Jang H, Plis SM, Calhoun VD, Lee J-H. Task-specific feature extraction and classification of fMRI volumes using a deep neural network initialized with a deep belief network: Evaluation using sensorimotor tasks. NeuroImage. 2017;145(Pt B):314-328.

6. Hoyer PO. Non-negative matrix factorization with sparseness constraints. The Journal of Machine Learning Research. 2004;5:1457-1469.

7. Calhoun VD, Adali T, Pearlson GD, Pekar JJ. A method for making group inferences from functional MRI data using independent component analysis. Human brain mapping. 2001;14(3):140-151.
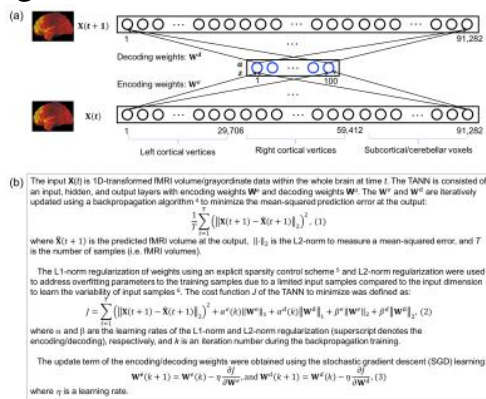
Figures

Figure 1. Temporal autoencoding neural network (TANN) to estimate underlying dynamics of the fMRI volumes: (a) network architecture and (b) learning algorithm. z and a are the input and output of the hidden nodes, respectively, and activation functions of the hidden and output nodes were tanh and linear, respectively. The MSMAll-preprocessed motor task fMRI from a subset of 897 subjects (n=50) in the HCP were used to reduce the computational load and resources during the training. The spatially smoothed (4mm isotropic Gaussian kernel in the grayordinates using the "wb_command –cifti-smoothing" function) data were also used to train the TANN.
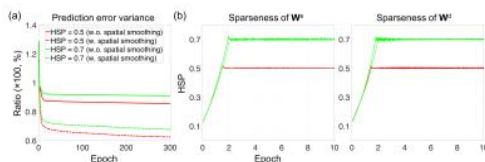

Figure 2. Learning curves of the (a) prediction error variance and (b) sparseness of the encoding weights (W^e) and decoding weights (W^d) of the TANN. The prediction error variances from the higher sparseness (i.e., HSP = 0.7) and using the unsmoothed fMRI volumes were higher than these from the lower sparseness and using the smoothed fMRI volumes. Both the encoding and decoding weights reached the target sparseness (i.e. HSP = 0.5 or 0.7) within few epochs. A total of 28,400 fMRI volumes (284 TRs/run × 2 runs/subject × 50 subjects; TR = 0.72s) were used per epoch. HSP, Hoyer's sparseness.
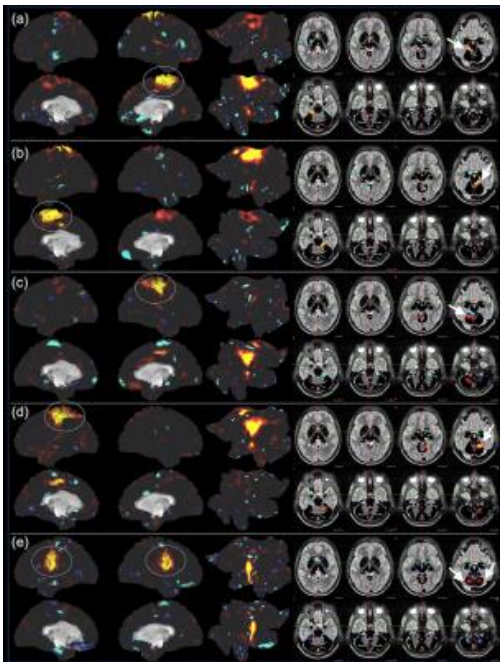
Figure 3. The highly task-specific feature maps of the decoding weights (i.e. $W^d_{(i)}$) from each of the (a) left-toe squeezing, (b) right-toe squeezing, (c) left-finger tapping, (d) right-finger tapping, and (e) tongue movements-related hidden nodes were shown. Brain regions with substantially high intensities in $W^d_{(i)}$ were marked using circles (cortical area) and arrows (subcortical/cerebellar areas). The TANN that presented these weight feature maps was trained using the smoothed fMRI volumes and when the HSP of weights was set to 0.7.
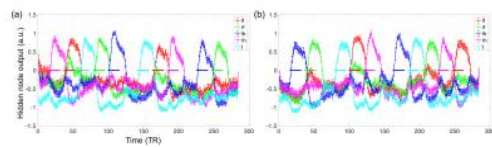

Figure 4. Output time-series (mean and standard errors across the 50 subjects) of the five hidden nodes of the trained TANN whose decoding weight features were shown in Fig. 3: using the fMRI data acquired from the (a) left-to-right and (b) right-to-left phase encoding directions (horizontal bars: task blocks). These time-series clearly illustrate the evolution of neuronal activations along the fMRI run, in which the participants performed each task across 2 blocks (12 s/block) followed by a visual cue in a run. lf, left-foot-toe clenching; rf, right-foot-toe clenching; lh, left-hand-finger tapping; rh, right-hand-finger tapping; t, tongue movement.
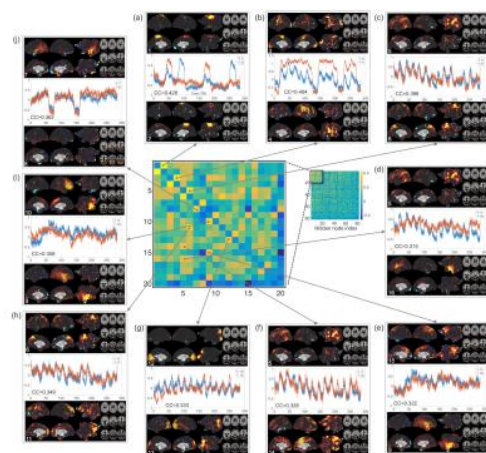

Figure 5. The 2D matrix of the temporal correlation coefficients (CCs) was calculated using the output time-series of the pairs of hidden nodes (center). The decoding weight features (i.e. parcellated neuronal networks) from the 10 paired hidden nodes representing the greater CCs were shown along with the output time-series of the corresponding hidden nodes (surround). The output time-series of these pairs of hidden nodes are substantially co-varying and thus the corresponding neuronal networks (i.e. decoding weights) are likely co-active during the task run.